Open Phys. 2015; 13:34–40 DE GRUYTER OPEN

Research Article Open Access

Ahti Niilisk*, Tauno Kahro, Valter Kiisk, Mihkel Rähn, Harry Alles, Jaan Aarik, and Väino Sammelselg

Raman modes in transferred bilayer CVD graphene

Abstract: A systematic experimental Raman spectroscopic study of twisted bilayer graphene (tBLG) domains localized inside wide-area single layer graphene (SLG) produced by low-pressure CVD on Cu foil and transferred onto SiO₂/Si substrate has been performed. According to the Raman characterization the tBLG domains had a great variety of twisting angles θ between the bottom and top graphene layers (6° < θ < 25°). The twisting angle θ was estimated from the spectral position of the rotating R and R' modes in the Raman spectrum. Under G band resonance conditions the breathing mode ZO with a frequency of 95– 97 cm⁻¹ was detected, and a breathing mode ZO was found in the spectra between 804 cm⁻¹ and 836 cm⁻¹, its position depending on the twisting angle θ . An almost linear relationship was found between the frequencies ω_{ZO} and ω_R . Also a few other spectral peculiarities were found, e.g. a high-energy excitation of the G band resonance, the 2G overtone appearing at 3170-3180 cm⁻¹ by the G band resonance, revealing a linear dispersion of 80 cm⁻¹/eV of the 2D band in tBLG

Keywords: chemical vapour deposition; graphene; twisted bilayer; Raman spectroscopy

PACS: 81.15.Gh, 68.65.Pq, 78.30.-j, 73.22.Pr

DOI 10.1515/phys-2015-0003 Received March 31, 2014; accepted August 05, 2014

Tauno Kahro: University of Tartu, Institute of Physics, Department of Materials Science, Ravila 14c, EE-50411 Tartu, Estonia

Valter Kiisk: University of Tartu, Institute of Physics, Department of Materials Science, Ravila 14c, EE-50411 Tartu, Estonia

Mihkel Rähn: University of Tartu, Institute of Physics, Department of Materials Science, Ravila 14c, EE-50411 Tartu, Estonia

Harry Alles: University of Tartu, Institute of Physics, Department of Materials Science, Ravila 14c, EE-50411 Tartu, Estonia

Jaan Aarik: University of Tartu, Institute of Physics, Department of Materials Science, Ravila 14c, EE-50411 Tartu, Estonia

Väino Sammelselg: University of Tartu, Institute of Physics, Department of Materials Science, Ravila 14c, EE-50411 Tartu, Estonia

1 Introduction

Since the early publications on misoriented graphene layers [1–3], twisted bilayer graphene (tBLG), a material with prospects for future electronics, has been the centre of great attention [4-9]. Among other characterization techniques such as scanning tunneling microscopy (STM), Landau level (LL) spectroscopy [6], high-resolution transmission electron microscopy (HRTEM) [10], optical microscopy and infrared spectroscopy, Raman spectroscopy has also been widely used in the studies of tBLG [10-29]. This is because Raman spectroscopy is a very sensitive and versatile tool to probe the electron-phonon and phononphonon coupling in graphene samples [11]. Raman spectra with intensive G and 2D peaks of single (SLG) and bilayer graphene (BLG) have been recorded most (e.g. [12-14]). In addition to the resonant G and 2D bands, the spectra also contain weak Raman peaks due to in-plane combination modes and overtones (LOTA, TOLA, LOLA, TOTA, and 2LO) [15-18]. The tBLG contains, besides the aforementioned spectral bands, out-of-plane modes such as breathing (ZO' and ZO [19–21]), rotation (R and R' [22–26]), and shear (C [27]) modes. Although these modes generally produce only weak Raman peaks compared with the G and 2D bands, they carry important information for characterizing the perfection, stacking order, and carrier transport in graphene samples.

As it is known [30-32], in BLG produced by mechanical exfoliation from HOPG, the bottom and top graphene layers primarily form a Bernal (or AB-) stack. AB-stacked bilayer graphene is characterized by two parabolic conduction and valence bands with zero bandgap between them [30–32]. In contrast, CVD graphene contains primarily tBLG, where the second graphene layer is rotated with respect to the first one. In tBLG, the low-energy electronic band structure can be represented by two Dirac cones separated by a wavevector that depends on the rotational angle [10, 13, 19]. Band-structure modifications and van Hove singularities in the energy dependence of the DOS (density of states) are induced when the Dirac cones of the top and bottom graphene layers are overlapping [6, 10]. There is a critical rotation angle of overlapping at which the given Raman excitation laser energy reaches the energy differ-

^{*}Corresponding Author: Ahti Niilisk: University of Tartu, Institute of Physics, Department of Materials Science, Ravila 14c, EE-50411 Tartu, Estonia, E-mail: Ahti.Niilisk@ut.ee

ence between the conduction and valence band van Hove singularities. This leads to a strong enhancement of the Raman G peak as well as to the changes in the 2D band position, intensity, and width [10, 13]. Also the out-of-plane modes, for example, the breathing mode ZO´ [19], are influenced by the resonance.

There are several works where the Raman properties of tBLG with respect to the rotation (twisting) angle between the layers have been studied [10, 13, 19, 20, 22-26, 33]. The twisting angle θ has been directly evaluated by using high resolution transmission electron microscopy (HRTEM) and scanning electron microscopy (SEM). As discussed by Carozo et al. [22] and Lu et al. [23] in the case of the tBLG superlattice at smaller twisting angles $3^{\circ} < \theta < 8^{\circ}$, a new R' band appears on the high-energy side of the intense G band in the Raman spectrum. The frequency of the R' band, $\omega_{R'} = 1625 \text{ cm}^{-1}$, can be assigned to the LO phonon branch with strong electron-phonon coupling close to the Γ point [22]. This R' mode is located in the same spectral range as the well-known defect band D', but is non-dispersive. Different from the D mode that shows a blueshift with the increase of laser energy [34], the spectral position of the R' mode does not change with laser excitation energy [22, 23]. In Ref. [23] it is stated that $\omega_{R'}$ increases monotonically as θ increases (for $\theta < 9^{\circ}$). Still, the $\omega_{\mathbb{R}'}(\theta)$ dependence is very weak and not clearly distinguishable (see e.g. [23]).

In the works [22, 23] it has been also shown that a new non-dispersive mode R emerges on the low-energy side of the G band for tBLG superlattice when the twisting angle θ increases. In Ref. [22] a weak R peak at $\omega_{\rm R} = 1435 \, {\rm cm}^{-1}$ was found for $\theta \approx 15^{\circ} \pm 2^{\circ}$. In the work by Campos-Delgado et al. [26] the R band position was determined for a medium θ interval (from 9° to 15°) and an interesting microscopic rainbow effect with θ was observed. In the works [22–24, 33] it was predicted and shown that at large twisting angles ($\theta > 20^{\circ}$) the R mode can be observed at Raman shift values down to 1370 cm⁻¹, where this band exists beside of the dispersive D band (or "D-like" band [24]). So, Wang et al. [25], using high-energy 364-nm UV-laser for G band resonance, specified the R ("folded TO") mode position for $\theta > 20^{\circ}$. Also, by using various laser excitations, they obtained a decrease of the folded phonon frequency with increasing θ in a wide range from below 10° to nearly 28°. In these works the R band was assigned to an intervalley double resonance scattering process; in momentum space it follows the transverse optical (TO) phonon branch, where the wavevector **q** changes along the highsymmetry $\Gamma \rightarrow K$ direction of graphene's Brillouin zone (Figure 1) [20, 22, 24, 25].

Among the other out-of-plane modes, the most attention

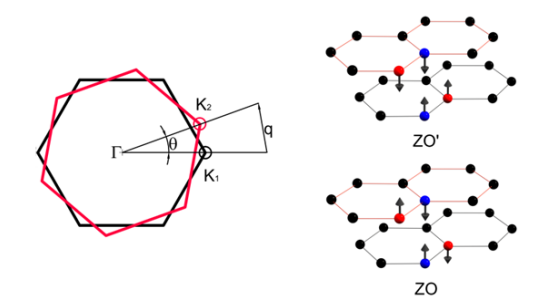


Figure 1: (left) Schematic zone diagram of the electronic band structure for tBLG with twisting angle θ . The high symmetry points K_1 and K_2 (Dirac points) for the first and second graphene layers are shown, respectively. \mathbf{q} is the wavevector of the tBLG superlattice. (right) Schematic of the lattice motion corresponding to the breathing modes ZO´ and ZO.

has been paid to the breathing modes ZO´ and ZO in tBLG (e.g. [19, 20], schematically see Figure 1). In the work by He *et al.* [19] a new mode at $94\,\mathrm{cm^{-1}}$ was ascertained under conditions leading to G band enhancement (resonance). They attributed this mode to the low-energy breathing mode (ZO´)_L, as high-energy breathing modes (ZO´)_H were also detected in a spectral range above $150\,\mathrm{cm^{-1}}$. The authors proposed that the (ZO´)_L phonons are activated by an intravalley double resonant process and the (ZO´)_H phonons are activated by the superlattice. As these modes were not seen in the AB-stacked BLG, the appearing of the breathing modes was facilitated here due to the lack of translational symmetry in tBLG [19].

Less is known about the other type of breathing mode, ZO. Together with the ZO breathing mode and other families of new bands, the ZO mode frequency was studied by Campos-Delgado *et al.* [20]; the authors have found this mode between 800–850 cm⁻¹ for various laser excitations.

Thus, the goal was to carry out a comprehensive Raman study of the tBLG domains localized inside wide-area single layer graphene produced by low-pressure CVD on Cu foils and transferred onto ${\rm SiO_2/Si}$ substrate. In the Raman scattering investigations various ${\rm Ar^+}$ -laser lines were used.

2 Samples and Experimental

Large-area graphene was grown on commercial 25- μ m thick polycrystalline copper foil (99.5%, Alfa Aesar) in a home-assembled CVD reactor. The foil was annealed for 40 min at 1000 °C in Ar/H₂ (both 99.999%, AS AGA Estonia) flow and then exposed to the flow of a mixture of

36 — A. Niilisk et al. DE GRUYTER OPEN

10% CH₄ (99.999%, AS AGA Estonia) in Ar at the same temperature for 45 min. Then the sample was cooled at the rate of 25 °C/min to room temperature in flowing Ar. The as-grown graphene film was transferred to a SiO₂/Si substrate (with 300 nm thick oxide layer) by using poly(methyl methacrylate) (PMMA; $M \sim 997000$, GPC, Alfa Aesar) as a supporting material. The copper foil was removed by an ammonium persulfate solution overnight. The floating PMMA/graphene film was rinsed using deionized water and transferred to SiO₂/Si substrate. The sample was dried in air and then heated on a hot plate to allow the PMMA reflow to improve the contact between the graphene and the substrate. The PMMA was then dissolved by dichloromethane (Alfa Aesar).

The transferred films consist of a quite perfect single graphene layer that sometimes had ruptures and wrinkled graphene stripes which emerges in the transferring process. Besides the predominant single-layer graphene (SLG) the samples contained also areas of tBLG with diameters up to 100 μ m. These darker areas were directly observable with optical microscope and were the main subject for the Raman measurements.

Raman scattering spectra were recorded with a Renishaw inVia confocal micro-Raman spectrometer. A 50° objective lens was used to focus the excitation beam of an Ar⁺ laser to an about 1 μ m spot on the sample, and to collect the backscattered Raman signal onto a Peltier-cooled CCD detector. Various Ar⁺-laser lines (514, 488, 458, and 364 nm) were used. The accumulation time varied from 10 s to about 1 hour depending on the intensity of the tBLG Raman mode. The radiant power was set to less than 1 mW in order to avoid a marked destroying effect on the graphene due to local heating. Spectral resolution was held at about $1\,\mathrm{cm}^{-1}$.

3 Results and discussion

3.1 Raman R' mode of bilayer graphene

First, in the bilayer part one can find domains which have in the Raman spectrum a sharp R' peak on the high-energy side of the G band, situated at $1622-1626 \text{ cm}^{-1}$, similar to the description in [22-24]. As an example in Figure 2 such a spectrum is shown for laser excitation at 488 nm. In the spectra with R' mode, the relative spectral intensities of the G and 2D bands do not vary much and the bands are relatively narrow. In the Raman spectrum we could not detect the breathing modes ZO' (inset in Figure 1) or ZO.

The relative intensity of the R band can change consid-

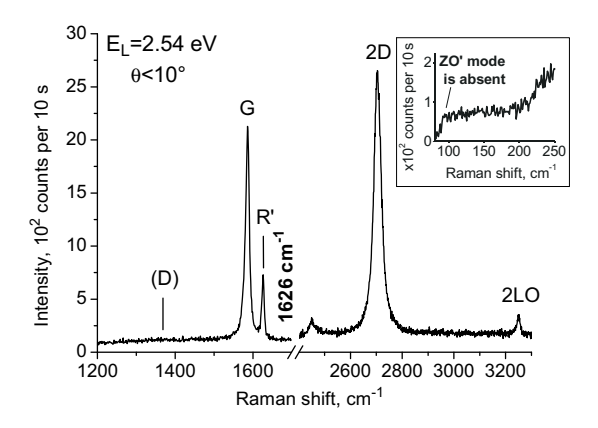


Figure 2: Raman spectrum with R' mode of a bilayer graphene having a small twisting (rotation) angle between the layers. Note the absence of the defect band D. The excitation wavelength was 488 nm. The inset demonstrates the lack of the breathing mode ZO'.

erably with respect to the G band. We have plotted the $S_{R'}/S_G$ ratio as a function of R' position in order to obtain additional information about the twisting angle θ in our tBLG samples. This is to some extent hindered due to the high relative intensity of the G band which lies at close proximity to the R' band as well as of the minute spectral shift of the latter. The result for two different laser lines is given in Figure 3. Regardless of the inexactness of the measurements, in both excitations (488 nm and 514 nm) some red shift of the R' band was obvious as the $S_{R'}/S_G$ ratio drops. The detected redshift of R' from about 1626 cm⁻¹ up to 1622 cm⁻¹ is very likely due to the decrease of the twisting angle θ . In Ref. [23] the Raman measurements gave the ratio of $S_{R'}/S_G = 0.18$ ($E_L = 2.54$ eV) for a twisting angle $\theta = 6^{\circ}$ as evaluated by HRTEM. This result fits well with our data on the $S_{R'}/S_G$ vs. $\omega_{R'}$ dependence (red point in Figure 3). As can be seen from Figure 2, we can attribute most of the measured spectra with R mode to the bilayer graphene with the twisting angle around 6° or less.

3.2 Raman R, ZO and ZO' modes of bilayer graphene under visible laser excitation

For tBLG with medium misorientation angles between the graphene layers, there are two characteristic features in the Raman spectra when excited at 514 nm or 488 nm. First, due to the band structure modification and the increasing possibility of intervalley transitions with the increasing twisting angle (e.g. [13, 14]), the Raman G band intensity may achieve a very high, resonant value, surpassing the integral intensity of the 2D band by several times. Secondly, in the case of the G band resonance the intensity

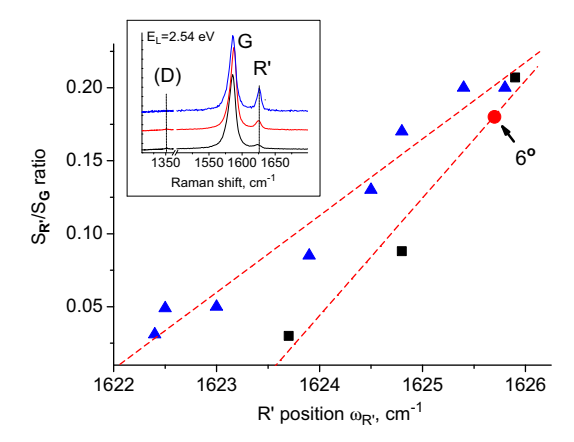


Figure 3: Integrated intensity ratio $S_{R'}/S_G$ versus R' peak position. The excitation wavelengths were 488 nm (black squares) and 514 nm (blue triangles). The red point is from Ref. [23]. The inset shows the R', G, and D band range in the Raman spectrum.

of the out-of-plane modes in Raman spectrum also considerably increases.

Representative Raman spectra measured with 488 nm laser excitation are shown in Figure 4. The most intense in the spectrum is the G mode: the peak intensities of the G and 2D bands differ by about a factor of 10. On the low-energy side of the G band a sharp peak appears which is attributed to the rotational R mode [20, 22, 24, 25]. This peak offers a possibility to determine the value of the angle θ from the Raman spectrum. Taking into account the reported $\omega_R(\theta)$ dependence (Figure 4d in Ref. [25]), for our sample with $\omega_R = 1486 \, \mathrm{cm}^{-1}$ (Figure 4), we get a value of $\sim 13^\circ$ for θ .

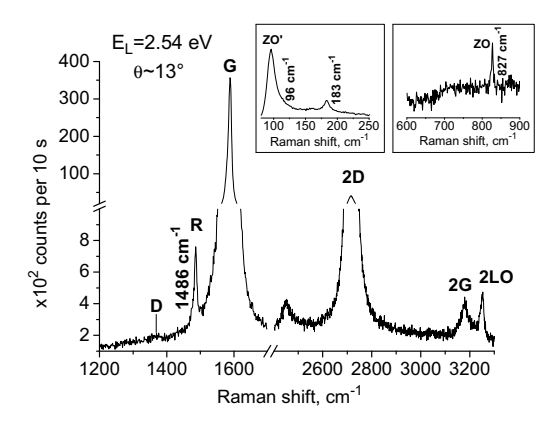


Figure 4: Raman spectrum with R mode of a bilayer graphene having a medium twisting angle between the layers. Note the minimal defect band D and the appearance of the 2G band. The excitation wavelength was 488 nm. Insets show spectra of the breathing modes ZO´ (left) and ZO (right). The axes are broken for clearer presentation.

Under conditions leading to G band enhancement, the breathing modes ZO´ and ZO also have their maximum intensity in Raman scattering (see insets in Figure 3). The ZO´ band (left inset in Figure 4) emerges in the Raman spectrum at frequencies below $100~\rm cm^{-1}$, beyond the effective spectral range of our Raman spectrometer, therefore the estimation of its exact spectral position is complicated. We found it to be at 95–97 cm $^{-1}$ and this agrees well with the result reported by He *et al.* [19]. In our experiments, the intensity of the ZO´ mode varied a lot, differing by (up to) 1–2 orders of magnitude. The rise and drop in the intensity of the ZO´ mode seemed to be in phase with the changes in the G band intensity, and thus connected with the θ variation among the measured graphene domains.

Noteworthy is that besides the low-energy ZO band, often in the Raman spectrum one can find weaker band(s) in the higher energy range (160–220 cm⁻¹, see also inset in Figure 4). More detailed discussion about these features remains open; they could be connected with the optical/acoustical branches ((ZO')_H, ZA) of the tBLG zone scheme [19, 20].

The ZO mode is positioned in Raman spectrum above $800\,\mathrm{cm^{-1}}$. In this spectral range the high background scattering from the $\mathrm{SiO_2/Si}$ substrate exists. To remove the background and to spot the weak ZO mode (about two orders less intense than the ZO mode), we subtracted from the Raman spectra the background obtained under the same conditions from SLG. In the resulting spectrum (right inset in Figure 4) the sharp peak of ZO mode is well visible.

It was found that the ZO mode position among the bilayer graphene domains varies a lot, from $804\,\mathrm{cm^{-1}}$ to $836\,\mathrm{cm^{-1}}$. Taking into account the recent results [20, 25] on the phonon dispersion in tBLG, we have plotted the ZO mode frequency ω_{ZO} versus the R mode position ω_{R} , and obtained very closely a linear dependence (Figure 5). Thus the spectral position of the ZO mode serves as an additional method for determination of the twisting angle in tBLG. In summary, taking into account the Raman data, we can estimate the observed θ interval in the tBLG domains, from about 10° to 16° , detectable with visible light excitation.

Finally, it is interesting to note that when the intensity of the G band has its highest value, a new high-energy band emerges in the range from 3170 cm⁻¹ to 3180 cm⁻¹. It is possible to attach this band to the overtone 2G or a combined mode G+ZO'+R. The peak position of this band may differ (can be less) from the sum of the G+G frequency value in a single measurement by up to 10 cm⁻¹. Nevertheless, it is possible to ascribe this band to the overtone 2G while the probability for the three-phonon process (G+ZO'+R) seems to be smaller. The 2G overtones were found earlier

38 — A. Niilisk et al. DE GRUYTER OPEN

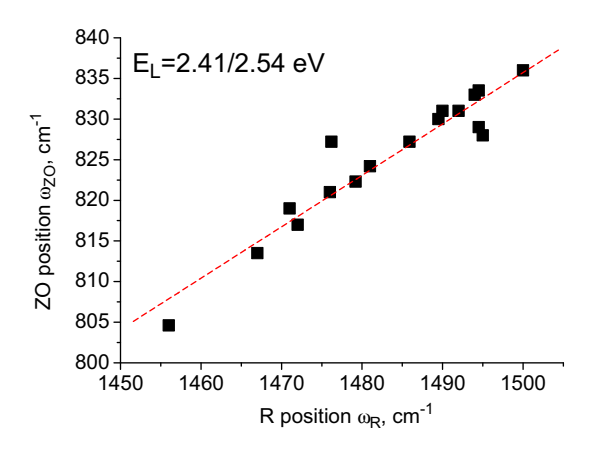


Figure 5: The spectral position of the breathing mode ZO versus the R (folded) phonon frequency. The black squares were obtained from Raman spectra of various tBLG domains in CVD graphene. Laser wavelengths 514 nm and 488 nm were used. A linear fit to the experimental data points is shown (red dashed line).

for SWNT (at $3182 \, \text{cm}^{-1}$) and MWNT (at $3175 \, \text{cm}^{-1}$) [34], as well as for a-C:H [35].

3.3 Raman modes of bilayer graphene under UV laser excitation

Increasing the twisting angle θ between the graphene layers leads to the situation where higher excitation energy is needed to generate the G band resonance and to observe the folded R mode in Raman spectra. This is demonstrated in Figs. 6 and 8 where the Raman spectroscopic signatures of tBLG with a large twisting angle are shown for two excitations (514 nm and 364 nm).

In Figure 6 the Raman properties of transferred SLG and BLG are shown in various spectral ranges. First, the integral intensity of two-layer graphene is strongly enhanced – 1.8 times for the G band and 2.5 times for the 2D band – as compared to SLG. Also the blueshift of about $10\,\mathrm{cm}^{-1}$ for the bell-shaped 2D band and its narrowing (FWHM is less than $30\,\mathrm{cm}^{-1}$) in the bilayer graphene is remarkable. These properties were discussed earlier by many authors.

In addition, by prolonged exposure it is possible to identify the known [15] in-plane combined LOTA, LOLA, and TOTA modes between 1850 to 2250 cm⁻¹ in both spectra. Their intensity and spectral background in tBLG are well enhanced compared with those of SLG; there exists also some relative blueshift of the combined modes (maybe due to their internal substructure [16]). However, no features in our tBLG spectra (Figure 7) can be detected in the range of out-of-plane modes, in the spectral region from

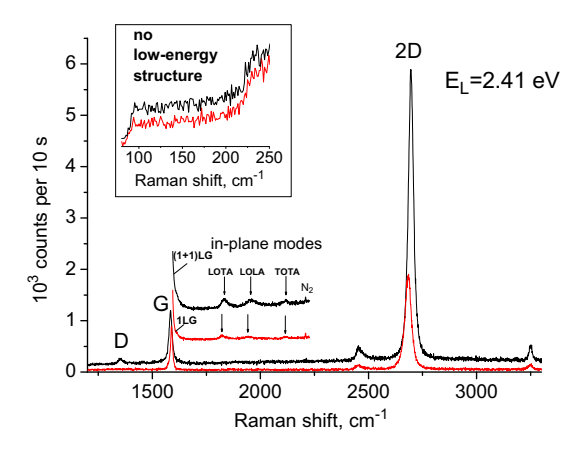


Figure 6: Comparison of the Raman features of SLG (red curves) and twisted BLG (black, referred as (1+1)LG) in a non-resonance situation ($\lambda_{exc} = 514$ nm). The relative changes in the G and 2D band areas are indicated. Also the in-plane phonons and lacking of ZO´ mode (inset) in both cases are shown.

1650 to 1850 cm⁻¹, where in the case of AB-stacked bilayer graphene the combined modes LOZA, LOZO', and 2ZO are situated [16–18]. Taking into account that in the spectrum of tBLG also the low-energy breathing mode ZO' is absent (inset in Figure 6), the situation by visible laser excitation is quite similar to that if this tBLG consists of two successive non-dependent single layers.

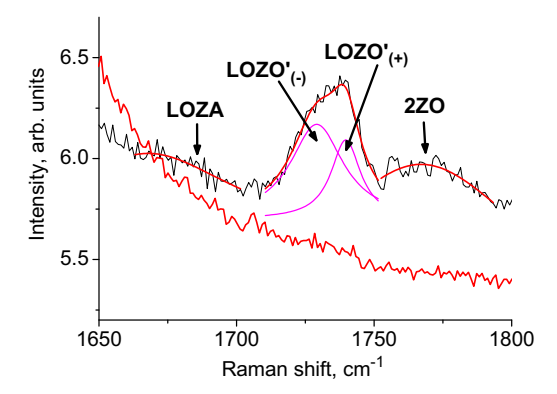


Figure 7: The presence and absence, respectively, of the out-ofplane modes in AB-stacked bilayer graphene (black curve) and tBLG (red curve). Smooth curves are Lorentzian fits of the peaks. The peaks are labelled after Ref. [18].

The situation greatly changes when using the UV-laser line which has excitation energy by about 1 eV higher compared to the visible laser. This change is seen in Figure 8 where Raman spectra from the same tBLG domain at two different excitations are presented. In the case of the 514 nm excitation ($E_{\rm L} = 2.41$ eV) we have an intense 2D band and a weaker G band, the integral intensity ratio

 $S_{\rm 2D}/S_{\rm G}$ being up to about 10. The defect mode D is represented weakly thus we have quite defect-free tBLG sample.

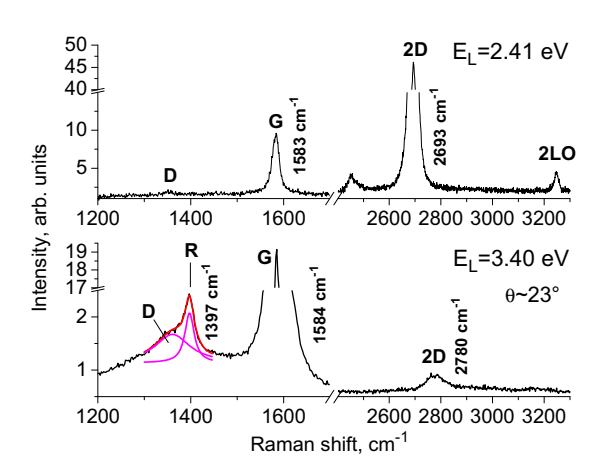


Figure 8: Raman spectra of tBLG excited at 514 nm (above) and 364 nm (below). In the latter case the G band resonance is achieved. The mode R is abstracted from the existing D band, its frequency yielding for $\theta \sim 23^\circ$ (estimated in accordance with data in [25]). Smooth curves are Lorentizan fits of the overlapping D and R peaks. The axes are broken for clearer presentation.

In constrast, by 364 nm laser excitation ($E_{\rm L}=3.40~{\rm eV}$, Figure 8 lower spectrum), there is a strong G band whereas the intensity of the 2D band is low. A ratio value of up to $S_{\rm 2D}/S_{\rm G}\approx0.1$ can be achieved. The defect mode D is considerably stronger and this band consists of two Lorentzian curves – it is possible to extract the R mode (Figure 8). So, we found the R peak at 1397 cm⁻¹ which corresponds to a twisting angle $\theta\approx23^{\circ}$, taking into account the folded mode vs. rotation angle dependence from Figure 4d in Ref. [25].

Regardless of the obvious enhancement of G band intensity under UV-excitation, we could not detect the breathing modes ZO´ or ZO in our Raman spectra. This may be due to the high level of defects generated by the UV laser in the graphene layers [25].

In Figure 8 a substantial blueshift of the 2D band frequency with laser energy is seen. It shifts on the average from 2693 cm⁻¹ to 2780 cm⁻¹ by the increase of the excitation energy from 2.41 eV to 3.40 eV, respectively, with reference to the dispersion properties of graphene. More detailed data about the 2D band shift with $E_{\rm L}$ is given in Figure 9 where experimental results $\omega_{\rm 2D}$ vs. $E_{\rm L}$ for four laser excitations are summarised. For tBLG we get a value of $d\omega/dE_{\rm L}=80~{\rm cm}^{-1}/{\rm eV}$ for the 2D band shift, which is reasonably less than that for the 2D band in SLG (100 cm⁻¹/eV [36]).

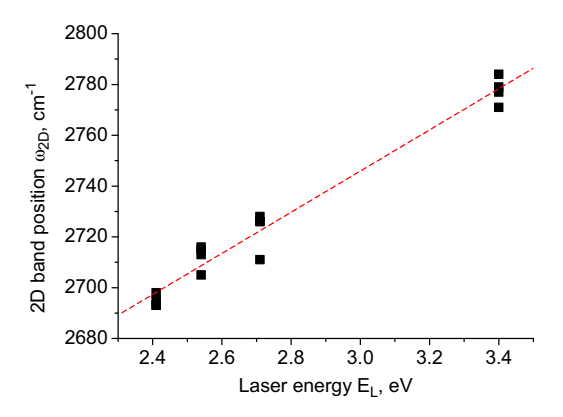


Figure 9: 2D band position vs. photon energy of the laser for different bilayer graphene samples. The red dashed line is a linear fit to the data.

4 Conclusions

We have performed a Raman spectroscopic study of the tBLG domains in CVD-grown single layer graphene on SiO₂(300 nm)/Si substrate by using various Ar⁺ laser excitations (514, 488, 458, and 364 nm) and found a great variety of Raman properties when switching from one tBLG grain to another. Besides the high-intense traditional G and 2D bands also several kinds of weaker spectral features were ascertained, the latter being more clearly expressed in the case of high G band intensity (resonance). These weaker modes in the spectra are of special interest because they are very informative for characterizing the perfection, stacking order, and also the carrier transport properties of graphene films. The twisting angle θ between the graphene layers in tBLG was determined considering the spectral position of the R and R' bands as also proposed earlier. We found tBLG domains with twisting angles between $6^{\circ} < \theta < 25^{\circ}$. By near-resonance conditions the breathing mode ZO' at 95–97 cm⁻¹ was also detected (compare with [19]). The weak breathing mode ZO was found in spectra between 804 cm⁻¹ and 836 cm⁻¹, its position depending on the twisting angle θ . An approximately linear run of the ZO phonon frequency with respect to the R peak position (and thus from the twisting angle θ) was established. This relation is reasonable as the corresponding ZO and TO phonon branches in momentum space have about even increments when the wavevector q changes along the high-symmetry $\Gamma \to K$ direction [28]. Also, other spectral peculiarities were found, for example a high-energy excitation of G band resonance, the emergence of the 2G overtone at 3170-3180 cm⁻¹ by the G band resonance, and revealing the linear dispersion of 80 cm⁻¹/eV of the 2D band in tBLG.

Acknowledgement: This research was carried out with the financial support of the European Social fund (Grant MTT1), Estonian Science Foundation (Grants Nos. 8666, 9283), Estonian Ministry of Education and Research (targeted projects SF0180046s07 and SF0180042s07) and the Graduate School "Functional materials and technologies" receiving funding from the European Social Fund under the project 1.2.0401.09-0079 in University of Tartu, Estonia.

References

- [1] J. Hass et al., Phys. Rev. B 75, 214109 (2007)
- [2] S. Latil, V. Meunier, L. Henrard, Phys. Rev. B 76, 201402(R) (2007)
- [3] J.M.B. Lopes dos Santos, N.M.R. Peres, A.H. Castro Neto, Phys. Rev. Lett. 99, 256802 (2007)
- [4] E.J. Mele, Phys. Rev. B 81, 161405 (2010)
- [5] S. Shallcross, S. Sharma, E. Kandelaki, O.A. Pankratov, Phys. Rev. B 81, 165105 (2010)
- [6] A. Luican et al., Phys. Rev. Lett. 106, 126802 (2011)
- [7] A.H. MacDonald, R. Bistritzer, Nature 474, 453 (2011)
- [8] J. Hicks et al., Phys. Rev. B 83, 205403 (2011)
- [9] A. Cocemasov, D. Nika, A. Balandin, Phys. Rev. B 88, 035428 (2013)
- [10] K. Kim et al., Phys. Rev. Lett. 108, 246103 (2012)
- [11] A.C. Ferrari, D.M. Basko, Nature Nanotechnology 8, 235 (2013)
- [12] Z.H. Ni et al., Phys. Rev. B 80, 125404 (2009)

- [13] R.W. Havener, H.L. Zhuang, L. Brown, R.G. Hennig, J. Park, Nano Lett. 12, 3162 (2012)
- [14] K. Sato, R. Saito, C.X. Cong, T. Yu, M.S. Dresselhaus, Phys. Rev. B 86, 125414 (2012)
- [15] K. Sato et al., Phys. Rev. B 84, 035419 (2011)
- [16] R. Rao et al., ACS Nano 5, 1594 (2011)
- [17] C. Cong, T. Yu, R. Saito, G.F. Dresselhaus, M.S. Dresselhaus, ACS Nano 5, 1600 (2011)
- [18] P.T. Araujo et al., Sci. Report 2, 1017 (2012)
- [19] R. He et al., Nano Lett. 13, 3594 (2013)
- [20] J. Campos-Delgado, L.G. Cançado, C.A. Achete, A. Jorio, J.-P. Raskin, Nano Research 6, 269 (2013)
- [21] C.H. Lui, T.F. Heinz, Phys. Rev. B 87, 121404(R) (2013)
- [22] V. Carozo et al., Nano Lett. 11, 4527 (2011)
- [23] C.-C. Lu et al., ACS Nano 7, 2587 (2013)
- [24] V. Carozo et al., Phys. Rev. B 88, 085401 (2013)
- [25] Y. Wang et al., Appl. Phys. Letters 103, 123101 (2013)
- [26] J. Campos-Delgado, G. Algara-Siller, C.N. Santos, U. Kaiser, J.-P. Raskin, Small 9, 3247 (2013)
- [27] P.H. Tan et al., Nature Matrials 11, 294 (2012)
- [28] P. Venezuela, M. Lazzeri, F. Mauri, Phys. Rev. B 84, 035433 (2011)
- [29] A. Righi et al., Phys. Rev. B 84, 241409 (2011)
- [30] Y.H. Ho, J.Y. Wu, Y.H. Chiu, J. Wang, M.F. Lin, Philos. Trans. R. Soc. Ser. A 368, 5445 (2010)
- [31] K.S. Novoselov et al., Nat. Phys. 2, 177 (2006)
- [32] Y.B. Zhang et al., Nature 459, 820 (2009)
- [33] A.K. Gupta, Y. Tang, V.H. Crespi, P.C. Eklund, Phys. Rev. B 82, R241406 (2010)
- [34] C. Thomsen, Phys. Rev. B 61, 4542 (2000)
- [35] A.C. Ferrari, J. Robertson, Phys. Rev. B 64, 075414 (2000)
- [36] M.A. Pimenta et al., Phys. Chem. Chem. Phys. 9, 1276 (2007)